Simulating the Effect of Periodic Nanopatterning on the Critical Temperature of Superconductors

THESIS

submitted in partial fulfillment of the
requirements for the degree of

BACHELOR OF SCIENCE
in
PHYSICS AND MATHEMATICS

Author :	Jasper van Egeraat
Student ID :	s1529374
Supervisor :	Milan Allan
2^{nd} supervisor :	Martina Chirilus-Bruckner

Leiden, The Netherlands, July 2, 2018

Simulating the Effect of Periodic Nanopatterning on the Critical Temperature of Superconductors

Jasper van Egeraat

Huygens-Kamerlingh Onnes Laboratory, Leiden University
P.O. Box 9500, 2300 RA Leiden, The Netherlands

July 2, 2018

Abstract

We describe a method to increase the critical temperature of BCS superconductors. The method is based on altering the electronic properties of a thin film of a superconductor by periodically fabricating holes in the crystal lattice. We use a MATLAB simulation to demonstrate that certain patterns enhance the coupling between electrons and phonons, which increases the transition temperature. In this project we attempted to improve the simulation such that it executes faster and is compatible with hexagonal structures.

Contents

Chapter 1

Introduction

Ever since the discovery of superconductivity scientists have searched for materials that superconduct at a higher temperature. It was long thought the phenomenon could only happen at a temperature below about 30 K. However, currently many materials have been discovered that superconduct at a temperature higher than even 100 K. Although these materials seem promising, the mechanism behind their high temperature superconductivity is unknown. These materials also often have a complex chemical structure, making them brittle and hard to manufacture on a large scale.

Luckily, there is a consistent theory describing the materials which only superconduct at temperatures below about 30 kelvin. These materials often have a simple chemical structure, making them easier to manufacture. For these reasons, it can be worthwhile to try to improve these low temperature superconducters rather than focussing on the high temperature superconductors.

By improving superconductors we mean to raise the lowest temperature at which the material superconducts. This critical temperature is denoted as T_c.

The way we will try to raise T_c is by periodic nanopatterning; changing the periodic crystal lattice by periodically removing atoms, thus changing the periodicity of the material. This will influence the electronic structure of the material, which in turns influences the critical temperature.

A MATLAB simulation is used to find what hole sizes and geometries will yield optimal results. This simulation has been created and used before and already provides promising results[1]. During this project, we have worked on improving the simulation. We have attempted to make the simulation run faster by converting some of the MATLAB code to C++, as C++ code has the potential to be faster than MATLAB code. Secondly,

we have tried to make the simulation compatible with hexagonal structures rather than only square lattices. Unfortunately we haven't met these goals, however we did make progress. In this thesis, we first provide the reader with some relevant theory, and then report on what has been tried to improve the simulation.

Chapter 2

Theory of superconductivity

In this section we will briefly touch on some of the related theory of superconductors.

2.1 BCS theory

Bardeen, Cooper and Schrieffer published the first microscopic theory of superconductivity in 1957. For this theory, which was named BCS theory after their names, they later recieved a Nobel prize as it was soon recognized to be correct in all essential aspects of low T_c superconductivity.

The theory is based on the following three assumptions for electrons in a solid material:

- The effective force between electrons can be attractive instead of repulsive.
- However weak this attractive force, electrons can form stable pairs.
- Under suitable circumstances, all electrons near the Fermi surface are bound in pairs. These electron pairs form a coherent state.

We shall now describe these assumptions and what implications they have.

Attractive electron interaction

It may be surprising to find an attractive interaction between electrons, since the Coulomb interaction tells us that like charges repel. To see how an attractive interaction is established, we consider an electron moving through the crystal lattice of a solid material. First, the repulsive force is

significantly reduced by screening due to the charged atoms in the lattice. Second, the electron can interact with phonons of the crystal lattice, by exciting one for example. Another electron can absorb this phonon and pick up the momentum. By interacting with phonons the resulting interaction between electrons can be attractive.

Electron pairs

Cooper discovered that this phonon mediated interaction between electrons in a solid material is attractive only near the Fermi surface. In fact, he found that for a single pair outside the Fermi sea the electrons form a bound state, due to this attractive interaction.

Coherent state

From the previous phenomenon followed that each electron on a Fermi surface is part of a pair. It should be noted that the bounded state of electron now behaves like a boson, since it has integer spin. Because of this and since there are a lot of such electron pairs in a material, the pairs overlap very strongly and form a highly collective condensate. From this follows that instead of looking at single electrons or pairs, the entire condensate should be taken into account.

The energy related to break a single pair is then related to the energy required to break all pairs in the condensate. Each bounded state in the condensate increases the energy barrier. At sufficiently low temperatures, the energy from collisions between atoms and electrons is not enough to break an electron pair. Because of this, the condensate as a whole does not interact with atoms anymore and it behaves like there are no atoms at all. Thus the atoms can't slow the electrons down, so the flow of the electron condensate experiences no resistance. This means the material is superconducting.

2.2 Second quantization

Throughout this thesis we will use the occupation number representation, which is also known as second quantization. This formalism is particularly convenient to describe quantum many-body systems.

In first quantization, a wave function of a many-body systems satisfies the following symmetry relation:

$$\Psi(r_1, r_2, \ldots, r_i, \ldots, r_j, \ldots, r_N) = \zeta\Psi(r_1, r_2, \ldots, r_j, \ldots, r_i, \ldots, r_N), \quad (2.1)$$

where r_i specifies the position of the i-th particle, and

$$\zeta = \begin{cases} 1 & \text{for bosons} \\ -1 & \text{for fermions} \end{cases}. \tag{2.2}$$

The wave function is here expressed in terms of position, but this symmetry property holds in any basis. Since it's impossible to tell identical quantum particles apart, this formalism isn't convenient because the wave function is expressed in terms of the properties of each particle. It is unphysical to ask what particle i is doing, because there is no way to keep track of the ith particle. For many-body systems the wavefunction also gets very tedious to work with.

Occupation number representation, or second quantization, is a different formalism which doesn't need this unphysical information and is more useful for calculations involving many-body systems. The starting point for this representation is the indistinguishability of identical particles[2].

We choose a complete and ordered single-particle basis $\{|\nu_1\rangle, |\nu_2\rangle, \dots\}$. With second quantization we can represent many-body states by writing how many particles are in each single-particle state. For example, states where n_{ν_1} particles are in the single-particle state $|\nu_1\rangle$, n_{ν_2} particles in $|\nu_2\rangle$, etc, can be represented as the ket $|n_{\nu_1}, n_{\nu_2}, \dots\rangle$.

It makes sense to introduce operators for the many-body state that raise or lower the amount of particles in a certain single-particle state. The annihilation operator c_{ν_i} and creation operator $c^\dagger_{\nu_i}$ lower and raise the occupation number of state ν_i respectively. It turns out that all operators, such as the Hamiltonian, can be written in terms of these operators. The ladder operators used to solve the Schrödinger equation for a harmonic oscillator are exactly annihilation and creation operators. We will use these kind of operators in the Hamiltonian in section 2.4.

2.3 Bloch's theorem

One of the most important results in solid state physics is Bloch's theorem. This theorem is a statement on the wavefunction of a particle in a periodic material*. More specifically, there is a basis of wavefunctions with the properties that each wavefunction ψ is an eigenstate and can be written as $\psi(\mathbf{r}) = e^{i\mathbf{k}\cdot\mathbf{r}}u(\mathbf{r})$, where u has the same periodicity as the crystal lattice of the material. Since electrons and the periodicity of the underlying crystal

*The periodicity comes from the underlying crystal lattice.

Version of July 2, 2018– Created July 2, 2018 - 13:07

lattice plays a big role in this project, and since this thesis is also submitted in partial fulfillment of the requirements for the bachelor of mathematics degree, we have done some additional research on this theorem. In this section, a (partial) proof is given of Bloch's theorem.

We first state for $N \in \mathbb{N}$ the N-dimensional (time independent) Schrödinger equation for the wavefunction $\psi : \mathbb{R}^N \to \mathbb{C}$ of a particle of mass $m \in \mathbb{R}_{>0}$ in a periodic potential $V(\mathbf{r}) : \mathbb{R}^N \to \mathbb{R}$. Thus we assume there are N linearly independent vectors $\mathbf{a_i} \in \mathbb{R}^N$ such that $V(\mathbf{r} + \mathbf{a_i}) = V(\mathbf{r})$. The N-dimensional parallelogram spanned by the vectors $\mathbf{a_i}$ will be denoted by A. The Schrödinger equation is an eigenvalue problem for the energy $E \in \mathbb{R}$ on an unbounded domain

$$\left[\frac{-\hbar^2}{2m}\nabla^2 + V(\mathbf{r})\right]\psi(\mathbf{r}) = E\psi(\mathbf{r}). \tag{2.3}$$

In this equation $\hbar$ is the reduced Planck constant. By substituting $q(\mathbf{r}) = \frac{2m}{\hbar^2}V(\mathbf{r})$ and $\lambda = \frac{2m}{\hbar^2}E$ we get the following equation on an unbounded domain:

$$\left[-\nabla^2 + q(\mathbf{r})\right]\psi(\mathbf{r}) = \lambda\psi(\mathbf{r}). \tag{2.4}$$

From now on we will call q the periodic potential. Throughout this section we assume that the potential is piecewise continous and that it has piecewise continuous first-order partial derivatives.

Theorem 2.3.1 (Bloch's Theorem)**.** *If λ is a real number such that* (2.4) *has a non-trivial bounded solution, then it has solutions of the form*

$$\psi(\mathbf{r}) = p(\mathbf{r})\exp(i\mathbf{c}\cdot\mathbf{r}) \tag{2.5}$$

where $p(\mathbf{r}) : \mathbb{R}^N \to \mathbb{C}$ is periodic with each vector $\mathbf{a_i}$ and $c \in \mathbb{R}^N$.

Note that equation (2.4) is a partial differential equation. Since these are often more difficult to work with, we will first consider some theory on ordinary differential equations. We will eventually provide the most important results for the 1 dimensional eigenvalue equation

$$\left(\frac{d^2}{ds^2} + q(s)\right)y = \lambda y, \tag{2.6}$$

where $y : \mathbb{R} \to \mathbb{R}$ and $q : \mathbb{R} \to \mathbb{R}$ are continuous. This is the one dimensional equivalent of (2.4), so equation (2.6) is an ordinary differential equation. The theory and results we will find can be extended to more dimensions, but this is not shown in this thesis. However, the theory for

ordinary differential equations is so enlightening that we will give that in the coming sections.

We will use the theory of linear operators to prove the theorem. Since differential operators are generally unbounded, we will actually focus on integral operators. As will soon be shown, differential equations can be reformulated as integral equations.

Before that we first provide the reader with some relevant definitions and theorems concerning linear operators in the coming sections. Some of these are taken directly from the book Linear Functional Analysis by Bryan P. Rynne and Martin A. Young[3], chapters 4, 6, 7 and 8. We will skip the proofs of most theorems, as these can be found in the book.

2.3.1 Basic definitions

This section serves to provide the most basic definitions which we will require.

Definition 2.3.2 (Hilbert space)**.** A Hilbert space is an inner product space which is complete with respect to the metric associated with the norm induced by the inner product.

The Hilbert space we will mostly use is the Lebesgue space $L^2[a, b]$.

Definition 2.3.3 (Linear operator)**.** Let X, Y be normed linear spaces and let $T : X \to Y$ be a linear transformation. If T is bounded, i.e. there exists a positive real number k such that $\|T(x)\| \leq k\|x\|$ for all $x \in X$, then T is called a linear operator.

Suppose X, Y are normed linear spaces. The set of all linear operators from X to Y is denoted by $B(X, Y)$. The set of all linear operators from X to X is denoted as $B(X)$. Note that a linear operator is bounded if and only if it's continuous.

Definition 2.3.4 (Spectrum)**.** The spectrum σ of a bounded operator T is the set of complex numbers μ such that $\mu I - T$ is not invertible.

It is in some sense a generalisation of the collection of eigenvalues of a matrix. A basic fact that we will see later is that a spectrum of a bounded operator is always closed.

Definition 2.3.5 (Adjoint operator)**.** Let $\mathcal{H}, \mathcal{K}$ be complex Hilbert spaces and $T \in B(\mathcal{H}, \mathcal{K})$. The unique operator $T^* \in B(\mathcal{K}, \mathcal{H})$ for which

$$(Tx, y) = (x, T^*y)$$

holds for all $x \in \mathcal{H}$ and all $y \in \mathcal{K}$ is called the adjoint operator of T. If $T \in B(\mathcal{H})$ then T is called self-adjoint if $T = T^*$.

For a proof of the existence and the uniqueness of an adjoint operator see [3].

Definition 2.3.6 (Compact operator)**.** Let X, Y be normed linear spaces. A linear map $T : X \to Y$ is compact if, for any bounded sequence $\{x_n\} \subset X$, the sequence $\{Tx_n\} \subset Y$ contains a convergent subsequence.

Theorem 2.3.7. *Suppose $\mathcal{H}$ is a complex Hilbert space, and $T \in B(\mathcal{H})$ a self-adjoint and compact bounded operator. Then T has finite non-zero eigenvalues. The set of non-zero eigenvalues is is either finite or consists of a sequence which tends to zero. Each non-zero eigenvalue is real and has finite multiplicity. The eigenvectors corresponding to different eigenvalues are orthogonal.*

This theorem implies that we can order the eigenvalues of a self-adjoint and compact operator T like $\lambda_1, \lambda_2, ...$

2.3.2 Integral operators

Let $\mathcal{H} = L^2[a,b]$. Let $R_{(a,b)} = [a,b] \times [a,b] \subset \mathbb{R}^2$, and $k : R_{(a,b)} \to \mathbb{C}$ a continuous function. For any $u \in \mathcal{H}$, define $f : [a,b] \mapsto \mathbb{C}$ such that

$$f(s) = \int_a^b k(s,t)u(t)dt.$$

It can be proven that for any $u \in \mathcal{H}$ the function f belongs to $\mathcal{H}$.

Definition 2.3.8 (Fredholm integral operator)**.** Let $\mathcal{H} = L^2[a,b]$. Let $R_{(a,b)} = [a,b] \times [a,b] \subset \mathbb{R}^2$, and $k : R_{(a,b)} \to \mathbb{C}$ a continuous function. Define $K : \mathcal{H} \to \mathcal{H}$ such that

$$Ku = \int_a^b k(s,t)u(t)dt \tag{2.7}$$

for $u \in \mathcal{H}$. It can be verified that the right hand side of this equation is indeed an element of $\mathcal{H}$. The operator is also linear and bounded. Then K is called the Fredholm integral operator, and k is called the kernel of K (not to be confused with the null-space of a linear operator).

An equation of the form $Ku = f$, where f is known and u unknown, is known as a first kind Fredholm integral equation. An equation of the form

$$(I - \mu K)u = f, \tag{2.8}$$

where $\mu \in \mathbb{C} \setminus \{0\}$, is known as a second kind Fredholm integral equation.

Theorem 2.3.9. *The integral operator $K : \mathcal{H} \to \mathcal{H}$ is compact.*

Theorem 2.3.10. *If the kernel k of an integral operator K is Hermitian, i.e. if $k(s,t) = \overline{k(t,s)}$ for all $s, t \in [a,b]$, then K is self-adjoint.*

2.3.3 Differential equations

The reason we stated the theory in the sections above is that it can be used for differential equations. Differential operators which arise are generally unbounded, which makes them problematic to work with. Instead it is possible to reformulate differential equations as integral equations, which give rise to integral operators which are bounded. In this thesis we will only consider a specific class of second order ODE's, but the methods can be extended rather easily.

Throughout this section we denote the set of continuous functions $f : [a,b] \to \mathbb{C}$ by $C[a,b]$. The subset of continuous functions on this domain whose first two derivatives are also continuous will be denoted as $C^2[a,b]$.

We consider the following ordinary differential equation on an interval $[a,b]$ where we assume $q, f \in C[a,b]$, together with boundary conditions

$$y''(s) + q(s)y(s) = f(s), \tag{2.9}$$
$$y(a) = y(b) = 0 \tag{2.10}$$

A solution is a function $y \in C^2[a,b]$. Let Y be the set of functions $y \in C^2[a,b]$ satisfying the boundary conditions $y(a) = y(b) = 0$, and define $T : Y \to C[a,b]$ by $Ty = y''$.

Lemma 2.3.11. *The map T is bijective. If $z \in C[a,b]$ then the solution $y \in Y$ to the equation $Ty = z$ is given by*

$$y(s) = \int_a^b g_0(s,t)z(t)dt \tag{2.11}$$

where

$$g_0(s,t) = \begin{cases} -\frac{(s-a)(b-t)}{b-a}, & \text{if } a \le s \le t \le b \\ -\frac{(b-s)(t-a)}{b-a}, & \text{if } a \le t < s \le b \end{cases}$$

Proof. Suppose $y \in Y$ and let $z = Ty$. By integrating this twice and substituting in the boundary conditions $y(a) = y(b) = 0$ we get equation (2.11).

To prove that T is injective, note that we can express $y \in Y$ in terms of $z = Ty$. Suppose $y_1, y_2 \in Y$ so that $Ty_1 = Ty_2 = z$ for some $z \in C[a,b]$. Then by equation (2.11) $y_1 = y_2$, so T is injective.

Suppose $z \in C[a,b]$ is arbitrary. Then define y by (2.11). It is easy to see that y can be differentiated twice and that is satisfies the boundary conditions $y(a) = y(b) = 0$. So $y \in Y$, and $Ty = z$. So T is also surjective. □

We let G_0 denote the integral operator defined by

$$G_0 z = \int_a^b g_0(s,t)z(t)dt$$

for $z \in C[a,b]$.

Lemma 2.3.12. *It holds true that $y \in C^2[a,b]$ is a solution of the differential equation* (2.9) *with boundary values* (2.10) *if and only if it satisfies the integral equation*

$$y = G_0(f - qy) \tag{2.12}$$

Proof. This follows from Lemma 2.3.11 by setting $z = f - qy$. □

With this lemma we see that the boundary problem (2.9), (2.10) is equivalent to the integral equation (2.12). This doesn't help us immediately to solve the differential equation, as we still need to solve an equation. However, we will show now that we are able to find an integral operator which will give us a solution to the differential equation immediately.

As an example, we assume $q = 0$ to get the following simple boundary value problem

$$y'' = f, \quad y(a) = y(b) = 0. \tag{2.13}$$

We can write this differential equation as $Ty = f$. It follows from lemma 2.3.12 the solution of (2.13) is directly given by $y = G_0 f$. Thus in a sense, T and G_0 are each others inverses. We call the operator G_0 for this problem a Green's operator, and the kernel g_0 is known as the Green's function.

As another example, we consider the eigenvalue problem

$$y'' = \lambda y, \quad y(a) = y(b) = 0. \tag{2.14}$$

So using the operator T this problem can be written as

$$Ty = \lambda y \tag{2.15}$$

From lemma 2.3.12 we find problem is equivalent to the eigenvalue equation

$$G_0 y = \frac{1}{\lambda} y. \tag{2.16}$$

So λ is an eigenvalue to the eigenvalue equation (2.14) if and only if $\frac{1}{\lambda}$ is an eigenvalue for G_0. The eigenfunctions are also similar, as the problems are equivalent. Since G_0 is an integral operator with a Hermitian kernel, we know by Theorem 2.3.9 and Theorem 2.3.10 that we can use the results from Theorem 2.3.7.

Integral operator for more general boundary value problem

We would now like to find an integral operator which gives us the solution to the more general boundary value problem

$$y'' + qy = f, \quad y(a) = y(b) = 0. \tag{2.17}$$

We assume $q, f \in C[a,b]$ and $y \in C^2[a,b]$. We will also consider the corresponding eigenvalue problem for when $f = \lambda y$.

It turns out that for a solution operator to exist there must be no non-zero solution to the homogeneous problem, i.e. 0 cannot be an eigenvalue to the eigenvalue problem.

Let y_l, y_r be solutions to the equation $y'' + qy = 0$, with the initial value conditions

$$y_l(a) = y_r(b) = 0,\ y_l'(a) = y_r'(b) = 1. \tag{2.18}$$

Lemma 2.3.13. *If 0 is not an eigenvalue to the eigenvalue problem for when $f = \lambda y$ in equation (2.17), there is a constant $C \neq 0$ such that $y_l(s)y_r'(s) - y_r(s)y_l'(s) = C$ for all $s \in [a,b]$.*

Proof. By differentiating $C(s) = y_l(s)y_r'(s) - y_r(s)y_l'(s)$ one sees this must be constant, and from the assumption that there is no non-zero solution to the homogeneous problem follows that the constant $C(s) = C \neq 0$. □

Theorem 2.3.14. *If 0 is not an eigenvalue to the eigenvalue problem for when $f = \lambda y$ in equation (2.17), then the function*

$$g(s,t) = \begin{cases} \frac{1}{C} y_l(s) y_r(t), & \text{if } a \leq s \leq t \leq b \\ \frac{1}{C} y_r(s) y_l(t), & \text{if } a \leq t < s \leq b \end{cases} \tag{2.19}$$

is a Green's function for the boundary value problem (2.17). Thus, for G the integral operator with kernel g the unique solution to (2.17) is given by $y = Gf$.

Proof. Let $y = Gf$. By using the definitions of g, y_l, y_r and differentiating twice it can be seen that y satisfies the boundary value problem (2.17). □

In the case that we have the eigenvalue problem $f = \lambda y$ we have the following two equivalent eigenvalue problems

$$\left(\frac{d^2}{ds^2} + q(s)\right) y = \lambda y, \tag{2.20}$$

$$Gy = \frac{1}{\lambda} y, \tag{2.21}$$

where G is defined as in Theorem 2.3.14. So λ is an eigenvalue to equation (2.20) if and only if $\frac{1}{\lambda}$ is an eigenvalue to equation (2.21). The eigenfunctions of (2.20) corresponding to λ are the same as the eigenfunctions of (2.21) corresponding to $\frac{1}{\lambda}$.

Theorem 2.3.15. *There are countably infinitely many eigenvalues for the boundary value problem*

$$\left(\frac{d^2}{ds^2} + q(s)\right) y = \lambda y, \quad y(a) = y(b) = 0. \tag{2.22}$$

We assume 0 *is not an eigenvalue. The eigenvalues can be ordered so that*

$$\lambda_1 > \lambda_2 > \dots,$$

and $\lambda_n \to -\infty$ *as* $n \to \infty$.

The set of corresponding eigenfunctions form an orthonormal basis for $L^2[a, b]$.

Proof. Let G be the integral operator as in theorem 2.3.14. The kernel g is symmetric, so hermitian. By Theorems 2.3.10 and 2.3.9, G is self-adjoint and compact. By Theorem 2.3.7 G has a countably infinite sequence of eigenvalues μ which tend to zero, and eigenvectors corresponding to eigenvalues form an orthonormal set. For each eigenvalue μ of G, there is an eigenvalue $\lambda = \frac{1}{\mu}$ for the boundary value problem (2.22). It follows naturally that the eigenvalues λ can be ordered as in the statement, and that the sequence converges to $-\infty$. The eigenfunctions of the integral operator are the same as the eigenfunctions for the boundary value problem (2.22), so by Theorem 2.3.7 the eigenfunctions form an orthonormal basis. □

2.3.4 Bloch's theorem

We now introduce the set S, called the conditional stability set. It consists of the values λ for which equation (2.4) has a non-trivial bounded solution.

We are now ready to work on a proof for Bloch's Theorem 2.3.1. We first state two eigenvalue problems related to equation (2.4).

Definition 2.3.16 (The periodic problem over $A(\mathbf{k})$)**.** Let $\mathbf{k} \in \mathbb{N}^N$ denote the N-tuplet $(k_1, k_2, \ldots, k_N)$. Let $A(\mathbf{k})$ be the N-dimensional parallelogram spanned by the vectors $k_1\mathbf{a_1}, k_2\mathbf{a_2}, \ldots, k_N\mathbf{a_N}$. Then the periodic problem over $A(\mathbf{k})$ is equation (2.4) considered to hold in $A(\mathbf{k})$ with the periodic boundary conditions

$$\psi(\mathbf{r} + k_j\mathbf{a_j}) = \psi(\mathbf{r}), \quad 1 \leq j \leq N. \tag{2.23}$$

Definition 2.3.17 (The **p**-periodic problem)**.** Let p_j $(1 \leq j \leq N)$ be real parameters such that for each j, $p_j \in (-1, 1]$. Let $\mathbf{p}$ denote the N-tuplet $(p_1, p_2, \ldots, p_N)$. The **p**-periodic problem is equation (2.4) considered to hold in A with boundary conditions

$$\psi(\mathbf{r} + \mathbf{a_j}) = \psi(\mathbf{r}) \exp(i\pi p_j), \quad 1 \leq j \leq N. \tag{2.24}$$

For both these two problems we can prove the existence of eigenvalues and corresponding eigenfunctions using Green's functions like in Theorem 2.3.15. To see the exact proof one can consult [4]. For now, we state the most important results of this method.

The eigenvalues of both problems are real and form a countably infinite set. We can denote the eigenvalues of the periodic problem over $A(\mathbf{k})$ as $\Lambda_n(\mathbf{k})$, and the eigenvalues of the **p**-periodic problem as $\lambda_n(\mathbf{p})$, where $n \in \mathbb{N}$. We have the following inequalities

$$\Lambda_0(\mathbf{k}) \leq \Lambda_1(\mathbf{k}) \leq \Lambda_2(\mathbf{k}) \leq \ldots, \tag{2.25}$$

$$\lambda_0(\mathbf{p}) \leq \lambda_1(\mathbf{p}) \leq \lambda_2(\mathbf{p}) \leq \ldots. \tag{2.26}$$

Both sequences converge to infinity as n goes to infinity. We let Σ denote the set of all $\Lambda_n(\mathbf{k})$ for $n \geq 0$ and $k_j \leq 1$ $(1 \leq j \leq N)$. The set of all $\lambda_n(p)$ for $n \geq 0$ and $-1 < p_j \leq 1$ $(1 \leq j \leq N)$ is denoted as $\mathscr{S}$.

For both sets of eigenvalues there is a corresponding set of orthonormal eigenfunctions. Let $\Psi_n(\mathbf{r}; \mathbf{k})$ denote the eigenfunctions of the periodic problem over $A(\mathbf{k})$, and let $\psi_n(\mathbf{r}; \mathbf{p})$ denote the eigenfunctions of the **p**-periodic problem. Thus we have

$$\int_{A(\mathbf{k})} \Psi_m(\mathbf{r}; \mathbf{k}) \Psi_n(\mathbf{r}; \mathbf{k}) d\mathbf{r} = \delta_{mn}, \tag{2.27}$$

$$\int_A \psi_m(\mathbf{r}; \mathbf{p}) \psi_n(\mathbf{r}; \mathbf{p}) d\mathbf{r} = \delta_{mn}, \tag{2.28}$$

$$\tag{2.29}$$

where δ is the Kronecker delta.

In the following theorem we show these two problems are somewhat related.

Theorem 2.3.18. *For each $1 \leq j \leq N$, let $r_j \in \{0, \ldots, k_j - 1\}$ and $-1 < p_{r_j} \leq 1$ be such that $\exp(i\pi p_{r_j})$ are the k_j-th roots of unity. So for each j there are k_j parameters p_{r_j}. Let $\mathbf{p_R}$ $(1 \leq R \leq k_1 k_2 \ldots k_N)$ denote the N-tuplets $(p_{r_1}, p_{r_2}, \ldots, p_{r_N})$ in any order. Then the set of all functions $\psi_n(\mathbf{r}; \mathbf{p_R})$ where $n \geq 0$, $1 \leq R \leq k_1 k_2 \ldots k_N$, and $\psi_n(\mathbf{r}; \mathbf{p_R})$ are solutions for the $\mathbf{p_R}$-periodic problem, is a complete set of eigenfunctions for the periodic problem over $A(\mathbf{k})$.*

Proof. We first show that the eigenfunctions $\psi_n(\mathbf{r}; \mathbf{p_R})$ satisfy relation (2.23). Since these eigenfunctions are solutions for the $\mathbf{p_R}$-periodic problem, we know that

$$\psi_n(\mathbf{r} + \mathbf{a_j}; \mathbf{p_R}) = \psi_n(\mathbf{r}; \mathbf{p_R}) \exp(i\pi \mathbf{p_{R_j}}). \tag{2.30}$$

Then

$$\begin{aligned}
\psi_n(\mathbf{r} + k_j \mathbf{a_j}; \mathbf{p_R}) =& \psi_n(\mathbf{r} + (k_j - 1)\mathbf{a_j}; \mathbf{p_R}) \exp(i\pi p_{R_j}) && (2.31)\\
=& \psi_n(\mathbf{r} + (k_j - 2)\mathbf{a_j}; \mathbf{p_R}) \exp(i\pi p_{R_j})^2 && (2.32)\\
=& \ldots && (2.33)\\
=& \psi_n(\mathbf{r} + (k_j - k_j)\mathbf{a_j}; \mathbf{p_R}) \exp(i\pi p_{R_j})^{k_j} && (2.34)\\
=& \psi_n(\mathbf{r}; \mathbf{p_R}). && (2.35)
\end{aligned}$$

So the eigenfunctions $\psi_n(\mathbf{r}; \mathbf{p_R})$ satisfy relation 2.23. The proof for the completeness can be found in [5]. □

To prove Bloch's theorem, we need two results from the spectral theory of differential equations. The differential operator associated with equation (2.4) is $L = -\nabla^2 + q(\mathbf{r})$ such that we have $L\psi(\mathbf{r}) = \lambda\psi(\mathbf{r})$. We let σ denote the spectrum of L.

Theorem 2.3.19. *Let λ be real such that equation* (2.4) *has a bounded solution. Then λ is in the spectrum σ.*

The proof can be found in [6].

Theorem 2.3.20. *For each $\mathbf{k}$, let σ_k denote the set of eigenvalues $\Lambda_n(\mathbf{k})(n \geq 0)$. Then λ is in σ if and only if $dist(\lambda, \sigma_k) \to 0$ as $k_1 \to \infty, \ldots, k_N \to \infty$.*

The proof of this theorem can be found in [4].

To recap, we now have the following 4 sets which we will require for the proof.

1. Σ, the eigenvalues of the periodic problem over $A(\mathbf{k})$, $k \in \mathbb{N}^N$,

2. $\mathscr{S}$, the eigenvalues of the **p**-periodic problem for $\mathbf{p} = (p_1, \ldots, p_N)$, $p_j \in (-1, 1]$,

3. σ, the spectrum of the differential operator L,

4. S, the conditional stability set.

Theorem 2.3.21. *The sets $\overline{\Sigma}$, $\mathscr{S}$, σ, and S are identical.*

Proof. Suppose $x \in \Sigma$. Then there are $\mathbf{k}$ and $n \in \mathbb{N}$ such that x is $\Lambda_n(\mathbf{k})$. Then, by Theorem 2.3.18, x is also the eigenvalue of some **p**-periodic problem. So $\Sigma \subset \mathscr{S}$.

Now suppose $y \in \mathscr{S}$. Let $\psi(\mathbf{r})$ be the corresponding eigenfunction, satisfying equation 2.24. Taking the absolute value of both sides gives $|\psi(\mathbf{r} + \mathbf{a_j})| = |\psi(\mathbf{r})|$ for all $(1 \leq j \leq N)$, which implies that ψ is bounded. This means that $y \in S$, so $\mathscr{S} \subset S$.

From Theorem 2.3.19 we see immediately that $S \subset \sigma$, so we have $\Sigma \subset \mathscr{S} \subset S \subset \sigma$.

Now suppose $z \notin \overline{\Sigma}$. Then by theorem 2.3.20 it is also not in the spectrum σ. Thus we have $\Sigma \subset \sigma \subset \overline{\Sigma}$. And since the spectrum σ is closed, by definition of the closure of a set this shows that the latter two sets are the same. Then all sets must be the same, so $\overline{\Sigma} = \mathscr{S} = S = \sigma$. □

We can now give the proof of Bloch's Theorem.

Proof. Since λ is in the conditional stability set S, by Theorem 2.3.21 it is also in $\mathscr{S}$. So there is a solution $\psi(\mathbf{r})$ and some **p** such that $\psi(\mathbf{r} + \mathbf{a_i}) = \psi(\mathbf{r}) \exp(i\pi p_j)$ for $1 \leq j \leq N$. Let **c** be the unique vector such that for all $1 \leq j \leq N$ we have $\mathbf{c} \cdot \mathbf{a_j} = \pi p_j$. Define $p(\mathbf{r}) = \psi(\mathbf{r}) \exp(-i\mathbf{c} \cdot \mathbf{r})$. It follows that $p(\mathbf{r})$ has period parallelogram A, and $\psi(\mathbf{r}) = p(\mathbf{r}) \exp(i\mathbf{c} \cdot \mathbf{r})$. □

The physical interpretation of the vector **c** is that it representents the wavevector of the particle. The most important take away from this section is that an electron in a periodic potential has eigenstates of the form $\psi(\mathbf{r}) = e^{i\mathbf{k}\cdot\mathbf{r}} u(\mathbf{r})$, where $u(\mathbf{r})$ has the same periodicity as the potential. Hence, this gives a means of quantifying how changing the periodic potential changes the eigenstates.

2.4 Hamiltonian

The Hamiltonian equation of our system we will consider consists of three parts:

$$H = H_{\text{el}} + H_{\text{ph}} + H_{\text{el-ph}}. \tag{2.36}$$

In the coming three sections we will discuss each part of the Hamiltonian.

2.4.1 Electron part of Hamiltonian

We approach the electronic structure of our material with the tight binding model. This model is based around the idea that the wavefunction of an electron in a material is a linear combination of atomic orbitals. For simplicity we assume there is only one orbital per atom and we make the approximation that orbitals are orthogonal to each other[†]. To clarify this model we start with a one dimensional monoatomic chain. The following sections closely follow the theory of [7]. For derivations of equations one can consult this source.

Monoatomic chain

Suppose we have N atoms in a chain where the spacing between atoms is the lattice constant a. We assume this chain has periodic boundary conditions, so that the n-th atom is the same as the $(n+N)$-th atom. We denote the orbital of the n-th atom by $|n\rangle$, so that our orthogonality condition is $\langle n|m\rangle = \delta_{nm}$. Then we use a general trial wavefunction of the form

$$|\Psi\rangle = \sum_n \phi_n |n\rangle , \tag{2.37}$$

where ϕ_n is the amplitude of the wavefunction $|n\rangle$. From this follows that for each atom n the effective Schrödinger equation takes form of the eigenvalue problem, where m sums over all atoms in the chain.

$$E\phi_n = \sum_m H_{nm}\phi_m, \tag{2.38}$$

where $H_{nm} = \langle n|H|m\rangle$ is the matrix element of the Hamiltonian. This matrix element is given by

$$H_{nm} = -\mu\delta_{nm} - t\delta_{(n,m)}, \tag{2.39}$$

where $\delta_{nm} = 1$ only when n and m are the same and $\delta_{(n,m)} = 1$ only when n and m are nearest neighbours. μ is the chemical potential of an electron in one of the orbitals, and t is called the hopping term. The physical

[†]When atoms are far apart, this approximation makes sense. But when the nuclei are close together, such as in the molecular structure of a solid, this approximation is far from correct. However, when not assuming orthogonality, improvements in accuracy do not justify the added complexity for our purposes.

interpretation of this is that this hopping term allows to move electrons from one atom site to another, but only when the sites are close enough, i.e. nearest neighbours.

Thus by plugging in equation 2.39 into equation 2.38 we get the following result:

$$E\phi_n = -\mu\phi_n - t(\phi_{n+1} + \phi_{n-1}). \tag{2.40}$$

By using an ansatz solution of the form $\phi_n = e^{-ikna}$, where k is the wavevector, it is fairly straight-forward to determine the energy spectrum. However this is not particularly enlightening for our current purposes.

Triatomic chain

Instead of a monoatomic chain, we will now consider a chain with a unit cell of 3 atoms which is represented as follows:

$$\ldots - x - y - z - x - y - z - \ldots \tag{2.41}$$

Each letter denotes a type of atom. We consider M unit cells, so that the total amount of atom sites is $3M$. Again we assume periodic boundary conditions, so that the j-th atom is the same as the $(j + 3M)$-th atom. This way we approximate a large (infinite) chain by using a small part of $3M$ atoms. For clarity we have shown 2 unit cells above. The distance between adjacent atoms is a, so the unit cell has a length of $3a$.

In the following, we let the index i represent the type of atom. In this case it is either x, y or z. Let ϕ_n^i be the amplitude of the wavefunction on the n-th site of atom type i.

We have an effective Schrödinger equation and Hamiltonian of the same type as the monoatomic case, however we have to be sure to take the different wavefunctions into account. By substituting the Hamiltonian into the Schrödinger equation we get the following 3 equations:

$$E\phi_n^x = -\mu_x\phi_n^x - t(\phi_n^y + \phi_{n-1}^z) \tag{2.42}$$
$$E\phi_n^y = -\mu_y\phi_n^y - t(\phi_n^z + \phi_n^x) \tag{2.43}$$
$$E\phi_n^z = -\mu_z\phi_n^z - t(\phi_{n+1}^x + \phi_n^y). \tag{2.44}$$

Like in the previous example for the monoatomic case, there is the chemical potential μ which is now dependent on the type of atom, and the hopping term t between nearest neighbours. Note that an electron on the n-th atom of type x can hop to either the n-th atom of type y, or to the atom of type z on the unit cell adjacent to it.

We now demonstrate the effect of substituting in the previous equations ansätz of the form

$$\phi_n^x = Ae^{ikn3a} \tag{2.45}$$
$$\phi_n^y = Be^{ikn3a} \tag{2.46}$$
$$\phi_n^z = Ce^{ikn3a}, \tag{2.47}$$

where k is the wavevector. This gives the following matrix equation after dividing common factors:

$$\begin{pmatrix} -\mu_x & -t & -te^{-in3a} \\ -t & -\mu_y & -t \\ -te^{in3a} & -t & -\mu_z \end{pmatrix} \begin{pmatrix} A \\ B \\ C \end{pmatrix} = E \begin{pmatrix} A \\ B \\ C \end{pmatrix} \tag{2.48}$$

We denote the matrix in this equation as $[H_k]$. It turns out that this matrix looks very similar in the case when we have more than 3 atoms in our unit cell. In fact, for a unit cell of $L \geq 3$ atoms, $[H_k]$ is a L by L matrix with chemical potentials on the diagonal, hopping terms on the super- and subdiagonal, and a hopping term with a phase factor in the upper right corner and the lower left corner.

In the coming sections we will call a unit cell consisting of more than 1 atom a supercell.

Tight binding Hamiltonian for lattice with supercell

We will now generalize the previous theory for mono- and triatomic chains to a lattice with square supercells with a size of L by L. Throughout this section we assume $L \geq 3$. We denote the number of supercells with M^2.

In the case of the triatomic chain, our matrix $[H_k]$ had diagonal elements with the chemical potentials of each of the 3 atoms, hopping elements between all adjacent elements, and an additional phase factor for connections between adjacent unit cells.

For a supercell of L by L we have the same elements, we just have to take into account the other dimension. Again we assume that the chemical potential depends on the type of atom. Let $\mathbf{K} = (K_x, K_y)$ be the reciprocal wavevector with respect to the periodicity of the supercell.

This leads to the matrices

$$[\mathbf{H_K}]^{\tau\tau'} = -\mu_\tau \delta_{\tau\tau'} - t(\delta_{(\tau,\tau')} + \delta_{(\tau,\text{up})} e^{-iLK_y} + \delta_{(\tau,\text{down})} e^{iLK_y} + \delta_{(\tau,\text{right})} e^{-iLK_x} + \delta_{(\tau,\text{left})} e^{iLK_x}), \tag{2.49}$$

where we use the single τ as an index of an atom. When τ and τ' represent the same atoms $\delta_{\tau\tau'} = 1$, and when τ and τ' are nearest neighbours $\delta_{(\tau,\text{left})} = 1$. $\delta_{(\tau,\text{up})} = 1$ when τ is nearest neighbour to a site in the next supercell to the right of it, and this is the similar for down, left and right. In all other cases the delta functions are 0.

Modelling holes

To model holes in the supercell, we need to do two things: increase the chemical potential of lattice points which make up the hole, and set hopping between holes and neighbours to zero. To achieve the latter we need t to be dependent on the lattice point indices. We get the following block Hamiltonians:

$$\begin{aligned}[\mathbf{H_K}]^{\tau\tau'} = &-\mu_\tau\delta_{\tau\tau'} - t_{\tau,\tau'}\delta_{(\tau,\tau')} - t_{\tau,\text{up}}\delta_{(\tau,\text{up})}e^{-iLK_y} - t_{\tau,\text{down}}\delta_{(\tau,\text{down})}e^{iLK_y} \\ &- t_{\tau,\text{right}}\delta_{(\tau,\text{right})}e^{-iLK_x} - t_{\tau,\text{left}}\delta_{(\tau,\text{left})}e^{iLK_x}\end{aligned}. \tag{2.50}$$

Second quantization representation of the electronic Hamiltonian

Using second quantization, the electron part of the Hamiltonian can now be written as

$$H_{\text{el}} = \sum_{\mathbf{K}} \mathbf{c}_{\mathbf{K}}^\dagger [\mathbf{H_K}] \mathbf{c}_{\mathbf{K}}, \tag{2.51}$$

where $\mathbf{c}_{\mathbf{K}}^\dagger, \mathbf{c}_{\mathbf{K}}$ are electron creation/annihilation operators.

2.4.2 Phonon part of Hamiltonian

The phonon part of the Hamiltonian is given by

$$\begin{aligned}H_{\text{ph}} = \sum_{\mathbf{r}} \frac{{\mathbf{p}_\mathbf{r}}^2}{2m} + \frac{\kappa}{2}\sum_{(\mathbf{r},\mathbf{r}')} (\mathbf{e_{nn}}\cdot(\mathbf{u_r} - \mathbf{u_{r'}}))^2 + \frac{\kappa'}{2}\sum_{[\mathbf{r},r']} (\mathbf{e_{nnn}}\cdot(\mathbf{u_r} - \mathbf{u_{r'}}))^2 \\ + \frac{\kappa''}{2}\sum_{\mathbf{r}} {\mathbf{u}_\mathbf{r}}^2.\end{aligned} \tag{2.52}$$

In the summations, $(\mathbf{r},\mathbf{r}')$ denotes nearest neighbours and $[\mathbf{r},\mathbf{r}']$ denotes the next nearest neighbours. κ, κ' and κ'' are spring constants. $\mathbf{p_r}$ and $\mathbf{u_r}$ are the momentum and the deviation of the atom at lattice site $\mathbf{r}$, respectively. $\mathbf{e_{nn}}$ is the unit vector in the direction of nearest neighbour, and

similarly $\mathbf{e_{nnn}}$ is the unit vector in the direction of the next-nearest neighbour.

This Hamiltonian results in the phonon spectrum. Although periodic nanopatterning can influence the phononic structure, for this project we focus on altering the electronic structure. Since according to BCS theory the critical temperature does not depend on the phononic structure as much as on the electronic strucure, we ignore the effect of periodic nanopatterning on the phonon spectrum.

2.4.3 Electron-phonon coupling part of Hamiltonian

The electron-phonon coupling Hamiltonian is responsible for the interaction between electrons and phonons. It is given by

$$H_{\text{el-ph}} = D \sum_{\mathbf{r}} \frac{\Delta V_{\mathbf{r}}}{V} c^{\dagger}_{\mathbf{r}} \mathbf{c_r}. \tag{2.53}$$

The displacement potential D represents the change of the chemical potential per volume change $\Delta V/V$. $c^{\dagger}_{\mathbf{r}}$ and $\mathbf{c_r}$ are electron creation and annihilation operators.

2.5 Determining the electron-phonon coupling constant λ

The effect of the electronic structure, phononic structure and the coupling between them on the critical temperature is summarized in the electron-phonon coupling parameter λ. BCS theory tells us that the relation between T_c and λ is given by

$$T_c \propto e^{-\frac{1}{\lambda}}. \tag{2.54}$$

In order to determine the parameter λ the Hamiltonian equations have to be diagonalized. From this the electron and phonon dispersion can be extracted.

The formula for λ of the pristine material is given by

$$\lambda^0 = \sum_{\mathbf{k},\mathbf{q}} \frac{2}{\omega_q N(0)} |g^0_{\mathbf{kq}}|^2 \delta(\epsilon_{\mathbf{k}}) \delta(\epsilon_{\mathbf{k}+\mathbf{q}}). \tag{2.55}$$

In this formula ω_q and ϵ_k are the phonon and electron dispersion, respectively. $N(0)$ is the electron density of states at the Fermi level. The two

delta functions are kinematic constraints and make sure that only states at the Fermi level are considered. The interaction matrix element $g^0_{\mathbf{kq}}$ has to do with the probability of the electron-phonon interaction. A high $g^0_{\mathbf{kq}}$ means that an electron with momentum $\mathbf{k}$ and a phonon with momentum $\mathbf{q}$ will interact more strongly. This in turn means that the electron can bond more strongly to another electron.

In the pristine material, the electron dispersion will be a single band. By supermodulating the material, we increase the periodicity, thus decreasing the size of the Brillouin zone and raising the number of bands. Because of this, there are more ways electrons can scatter, since there are more bands and we now take scattering between different (reduced) Brillouin zones into account. By designing the supercell we can influence how the electrons scatter. With supermodulation we want to make sure that electrons will easily scatter at points with a high interaction matrix element $g^{\nu\nu'}_{\mathbf{kq}}$. The superscripts ν and ν' indicate the band indices.

The formula for λ of the supermodulated material is then given by

$$\lambda^{\text{new}} = \sum_{\mathbf{k},\mathbf{q},\nu,\nu'} \frac{2}{\omega_{\mathbf{q}} N(0)} |g^{\nu\nu'}_{\mathbf{kq}}|^2 \delta(\epsilon^{\nu}_{\mathbf{k}}) \delta(\epsilon^{\nu'}_{\mathbf{k}+\mathbf{q}}), \tag{2.56}$$

where we now also sum over the different bands.

Version of July 2, 2018– Created July 2, 2018 - 13:07

Chapter 3

Improving the MATLAB simulation

This project uses a MATLAB simulation to compute the effects of periodic nanopatterning on the parameter λ. Creating the numerical simulation was not part of this project as the simulation was already created[1]. During our project we have worked on improving this simulation. We have attempted to shorten computation time by converting certain segments of the code to C++ and we tried to make the simulation compatible with hexagonal lattices. The efforts are described in this chapter, but first we give a short introduction to the MATLAB simulation.

3.1 Implementation of the theory

This chapter briefly describes the outline of the MATLAB code. As an input, the code requires several parameters to construct the model. The most relevant are summarised here:

- L, the periodicity of supermodulation
- M, the amount of unit cells
- a, the lattice constant
- the hole shape
- the spring constants (see equation (2.52))
- the electron-phonon coupling strength

- μ, the tight binding energy constant
- t, the hopping constant

From this the matrices $[\mathbf{H_k}]$ as in equation (2.50) are computed. This gives the electronic structure, from which eventually the parameter λ can be determined, as in equation (2.56). It then compares this λ^{new} to the λ^0 of the pristine material. The output of the simulation is the ratio between the two λ's. The simulation can also provide the user with graphs of the electronic band structure among other things.

3.2 Improving computation speed

Although MATLAB is fast with matrix multiplications, an efficient programmer could save computation time when writing C++. Especially with long nested loops C++ can be a faster alternative. As the simulation makes use of a couple nested loops, an investigation is made to find out if converting MATLAB code to C++ will be able to shorten computation time.

For small unit cells of about 6 by 6, the simulation is very quick, determining λ for a given hole in a matter of seconds. However, for bigger supercells, such as 20 by 20, the simulation becomes very slow, and determining λ now takes up to a couple hours. Therefore, as part of this project an attempt is made to write certain parts of the simulation in C++, so as to speed up the computation time for these big supercells.

One can write C++ programs which interact with MATLAB using MEX functions. By using the C++ MEX API and after compiling the code using MATLAB, one can call the C++ program as if it were an ordinary MATLAB function. Since the C++ code can get input from MATLAB and return output to MATLAB, this seemed useful for our current goal.

We ran into the following things during this part of the project:

- Reading MATLAB input is slow. Since some data had to be accessed multiple times, it was faster to first put MATLAB input into regular C++ variables, and then use that variable. This saved a lot of time.
- MATLAB crashes when the C++ program uses too much memory. This poses a problem for big enough unit cells.
- MATLAB uses very efficient libraries to calculate matrix multiplications. The C++ code which was produced for this project does not use libraries for matrix multiplication, but rather uses brute force to

compute the result. Much time could probably be saved using efficient libraries.

Since not each step the simulation carries out becomes very slow for big unit cells, we targeted a part which contains a quadruple nested loop. This section becomes very slow for larger unit cells.

To see whether using MEX functions as a means to cut computation time is feasible, we first decided to compare computation speed of quadruple nested for loop, without adding any interesting computations within the loops. For a 6 by 6 supercell this looked like this:

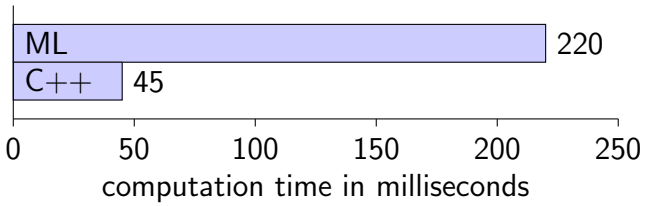

From this it would seem that MEX functions can be used to speed up the original quadruple nested loop. Also for bigger supercells C++ is a lot faster than MATLAB. After translating the original MATLAB code to C++ we compare it to find the following for a 6 by 6 supercell.

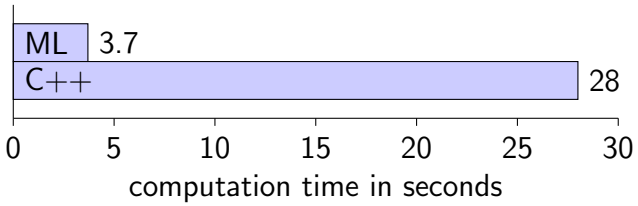

Unfortunately it is quite slower in C++, and for bigger unit cells the difference between computation speed only becomes bigger. This is probably due to inefficient coding. We suspect a more experienced programmer would be able to decrease computation speed of the C++ code, perhaps to the point that it is faster than MATLAB.

3.3 Lattice types

Currently, the simulation works only for square lattices. However, many materials that can be manufactured as a very thin sheet have a hexagonal structure. Therefore, as part of this project, an attempt is made to extend the simulation so that it is compatible with hexagonal structures.

3.3.1 Square lattices

In an effort to understand how to make the simulation compatible with hexagonal structures, we first expand on the square lattice to gain a better understanding about the things that we need to change.

As explained in section 2.4.1 we have the following matrices that need to be diagonalized for each wavevector $\mathbf{K}$:

$$\begin{aligned}[\mathbf{H_K}]^{\tau\tau'} = &-\mu_\tau\delta_{\tau\tau'} - t_{\tau,\tau'}\delta_{(\tau,\tau')} - t_{\tau,\text{up}}\delta_{(\tau,\text{up})}e^{-iLK_y} - t_{\tau,\text{down}}\delta_{(\tau,\text{down})}e^{iLK_y} \\ &- t_{\tau,\text{right}}\delta_{(\tau,\text{right})}e^{-iLK_x} - t_{\tau,\text{left}}\delta_{(\tau,\text{left})}e^{iLK_x}\end{aligned} . \tag{3.1}$$

To clarify how this matrix looks, we show a part of a square lattice where we have a 3 by 3 unit cell in figure 3.1. In this figure, each circle represents an atom. The orange lines indicate a horizontal connection between adjacent atoms, the green lines indicate a vertical connection between adjacent atoms. We represent connections between neighbouring unit cells with blue lines.

The form of the accompanying Hamiltonian $[\mathbf{H_K}]$ matrix is as shown in figure 3.2. The numbers on top and on the left represent the atoms as in 3.1. So a connection from atom 2 to atom 5 in figure 3.1 is represented by the entry in the 2nd row and the 5th column in figure 3.2. The black dots along the diagonal represent the chemical potential term μ. The green and orange dots are the hopping terms t between adjacent atoms within a supercell, the color depending on the direction as in figure 3.1. Since the terms associated with hopping to adjacent supercells depend on the direction, these are represented by blue arrows. These will get the phase factor corresponding to the direction as in equation 3.1.

To model holes, hopping terms to and from sites that represent holes are then set to zero and the chemical potential of these hole sites is increased.

The matrix $[\mathbf{H_k}]$ is to be diagonalized in the simulation for each wavevector k. We suspect that these matrices are the only thing that need to be updated to make the simulation compatible with hexagonal structures.

3.3.2 Hexagonal lattices

To determine how the matrices $[\mathbf{H_k}]$ look for a hexagonal lattice we first show a part of a hexagonal lattice with a 3 by 3 supercell in figure 3.3. From this figure it can be seen that in a hexagonal lattice, each atom has 6 nearest neighbours instead of the 4 in a square lattice. Furthermore, in the square lattice connections could either be horizontal or vertical. Connections in

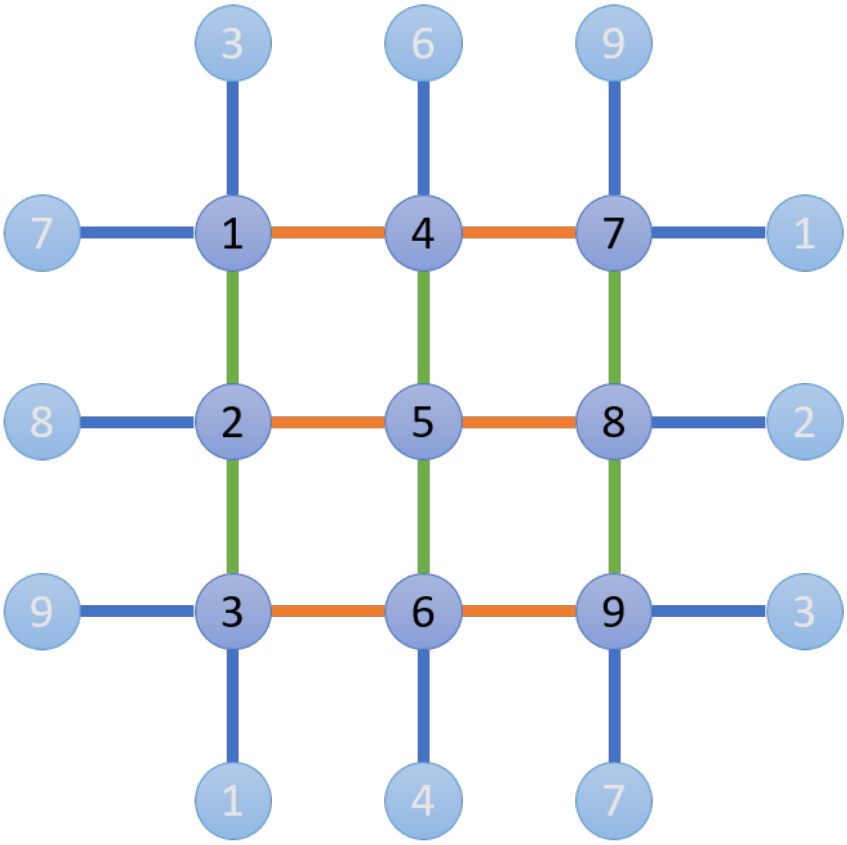

Figure 3.1: *A 3 by 3 unit cell in a square lattice.*

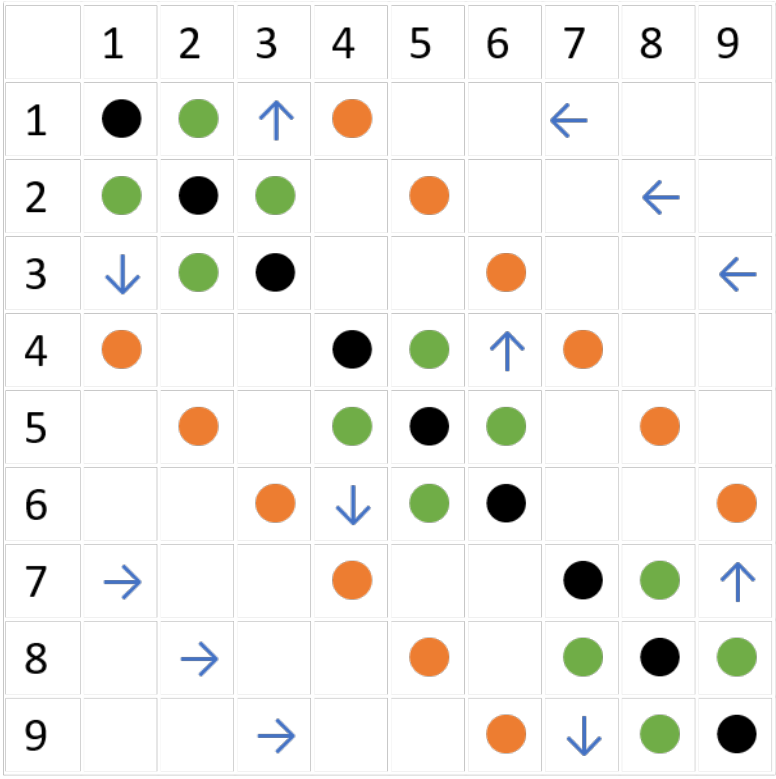

Figure 3.2: *The Hamiltonian matrix* $[\mathbf{H_k}]$ *for a 3 by 3 unit cell in a square lattice. The colors of entries correspond to the colors of directions in figure 3.1.*

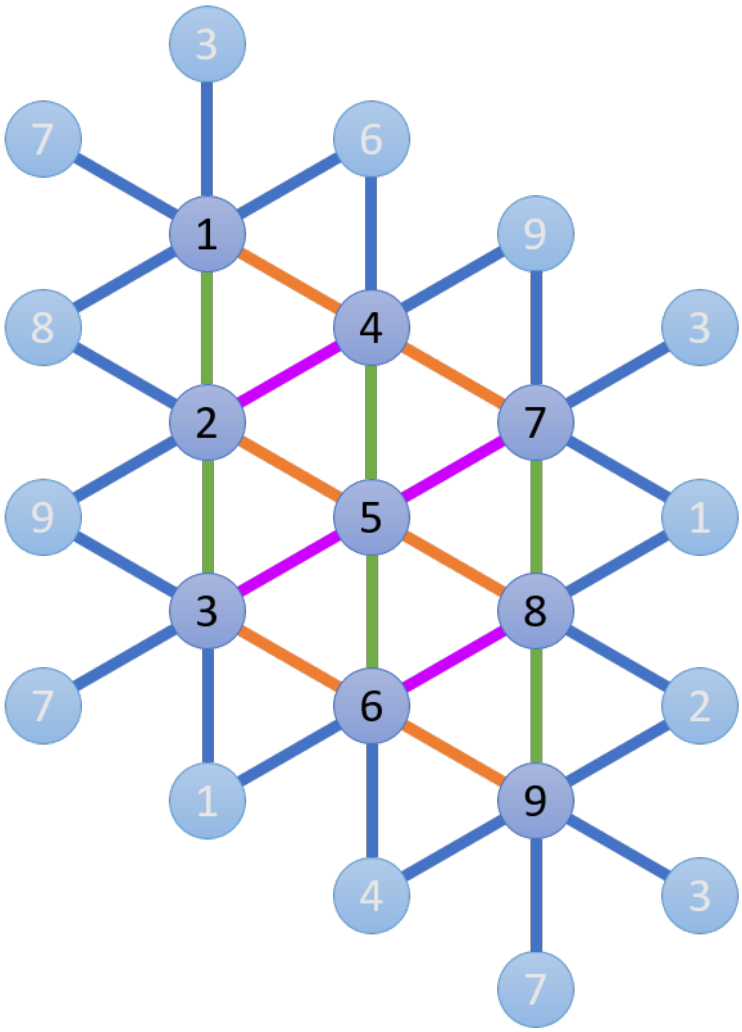

Figure 3.3: *A 3 by 3 unit cell in a hexagonal lattice.*

Figure 3.4: *The Hamiltonian matrix for a 3 by 3 unit cell in a hexagonal lattice. The colors of entries correspond to the colors of directions in figure 3.3.*

the hexagonal structure can be in 3 directions. Again vertical connections are represented with green lines. Tilted connections are either orange or purple. Connections between neighbouring unit cells are denoted with a blue line.

Taking into account the extra nearest neighbours and the different directions of skewed connections, we show our speculation of the Hamiltonian matrices $[\mathbf{H_K}]$ in figure 3.4. Again the numbers on top and on the left represent the atoms as in figure 3.3. The black dots along the diagonal represent the chemical potential term μ. The green, orange and purple dots are the hopping terms t between adjacent atoms within a supercell, the color depending on the direction as in figure 3.3. Again the terms associated with hopping to adjacent supercells are represented by blue arrows in the direction of the connection. These entries get a phase factor depending on this direction. The exact factor follows from simple geometry; e.g. the phase factor for the connection from atom 7 in the supercell to atom 3 in

the adjacent supercell is

$$\exp(-i\left(\frac{\sqrt{3}}{2}K_x + \frac{1}{2}K_y\right)L). \tag{3.2}$$

Implementation

To fully understand the problems posed in this section, we recommended the reader to refer to the MATLAB code.

Before implementing this, we ran into a problem concerning the phase factors in the square lattice. It seemed that the direction of phase vectors was 90 degrees of. For example, entries that are supposed to connect to the unit cell upwards actually got a phase vector corresponding to a connection to the unit cell right. Despite this, it gave consistent results, and changing the directions so that they would seem more logical gave wrong results.

We first tried to implement the matrix corresponding to the hexagonal lattice with the phase vectors 90 degrees shifted. This produced nonphysical results, so we decided to try to find out why phase vectors should be rotated by 90 degrees in the square lattice. This might provide more insight on how to determine the correct phase directions for the hexagonal structure.

A possible explanation is that the lattice ordering used to be different than the linear indexing in MATLAB. The lattice used to be ordered as

$$\begin{pmatrix} 1 & 2 & 3 \\ 4 & 5 & 6 \\ 7 & 8 & 9 \end{pmatrix}. \tag{3.3}$$

In MATLAB, one can access matrix entries by single index. When you index a matrix by using only one subscript, MATLAB treats it as if its elements are in a long column vector, by going down the columns consecutively. The linear indices for a matrix are according to this ordering

$$\begin{pmatrix} 1 & 4 & 7 \\ 2 & 5 & 8 \\ 3 & 6 & 9 \end{pmatrix}. \tag{3.4}$$

The MATLAB simulation actually uses this type of indexing in determining what elements needed what type of phase factor. By transposing the original lattice ordering, the atom number corresponds to the single index. The lattice ordering is actually not used by the simulation in calculations,

and is only there for us to gain better insight. This made things easier to comprehend, and it turned out that using this transposed lattice ordering the matrix entries of $[\mathbf{H_k}]$ that correspond to vertical connections are correct. However, matrix entries that correspond to horizontal connections are now mirrored.

Unfortunately I could not find an explanation as to why these entries should remain mirrored*. However, implementing the Hamiltonian matrix $[\mathbf{H_k}]$ using the new notion that horizontal directions should be flipped, provided results which would seem incorrect.

The simulation calculates the coupling parameter λ without supermodulation and with supermodulation and then compares. When testing with a supercell with no holes, we should see no change in λ. For testing with a 3 by 3 supercell with no holes, we unfortunately get a λ decrease of -41.8%.

Whether the current implementation of the matrix $[\mathbf{H_k}]$ for the hexagonal lattice is incorrect or whether more changes need to be made to the simulation is unknown at this time. It would be helpful to do a study on band structures for hexagonal materials before tackling this problem, to see whether results are correct or incorrect. Due to time constraints this has not been done during this project.

*Mirroring the horizontal phase vectors again would give incorrect results.

Chapter 4

Discussion on the future of this project

During this project, our main goal was improving the simulation. At first an attempt was made to decrease computation time. We also tried making the simulation compatible with hexagonal structures.

We didn't manage to decrease computation time. Perhaps a more experienced coder would be able to improve the execution speed by programming more efficiently.

It should be taken into account that currently the simulation is able to provide data supporting the concept that supermodulation in materials with a square lattice can improve the critical temperature of superconductivity, with an acceptable execution time. The computation speed might be slow to find hole size and parameters which optimise the electron-phonon coupling parameter λ, however it is quick with determining whether a given hole size and geometry will improve it.

Effort was also made to make the simulation compatible with hexagonal materials. So far, this has not worked yet. There was not enough time to fully understand why the phase factors seemed to be in incorrect directions. With more time it would also be helpful to do research on how band structures should look for hexagonal lattices, before looking into this problem. Since many nearly 2D materials have hexagonal structure, it is worth to pursue solving this problem to find whether making holes in these structures can improve the critical temperature. After all, there is a chance that periodic nanopatterning does not work for hexagonal lattices.

At this time, there is no experimental proof yet that periodic nanopatterning in superconductors will actually improve the critical temperature. It may be worthwhile to experimentally test this before working on a bet-

ter version of the simulation, as currently it is already able to provide promising results.

Bibliography

[1] M. Allan, M. H. Fischer, O. Ostojic, and A. Andringa, *Creating better superconductors by periodic nanopatterning*, SciPost Physics **3** (2017).

[2] H. Bruus and K. Flensberg, *Many-body quantum theory in condensed matter physics: an introduction*, Oxford university press, 2004.

[3] B. P. Rynne and M. A. Youngson, *Linear functional analysis*, Springer Science & Business Media, 2000.

[4] E. C. Titchmarsh and T. Teichmann, *Eigenfunction Expansions Associated with Second-Order Differential Equations, Part 2*, Physics Today **11**, 34 (1958).

[5] M. S. P. Eastham, *The spectral theory of periodic differential equations*, Scottish Academic Press [distributed by Chatto & Windus, London, 1973.

[6] I. Glazman, I. M. Glazman, I. M. Glazman, S. U. Mathematician, I. M. Glazman, and U. S. Mathématicien, *Direct methods of qualitative spectral analysis of singular differential operators*, Israel program for scientific translations, 1965.

[7] S. H. Simon, *The Oxford solid state basics*, OUP Oxford, 2013.